J. Plasma Fusion Res. SERIES, Vol. 5 (2002) 42–49

Resistive Wall Mode Control on the DIII-D Device

OKABAYASHI Michio, BIALEK James[1], CHANCE Morrell, CHU Ming[2], FREDRICKSON Eric, GAROFALO Andrea[1], HATCHER Ronald, JENSEN Torkil[2], JOHNSON Larry, LA HAYE Robert[1], LAZARUS Edward[3], MANICKAM Janardhan, NAVRATIL Gerald[1], SCOVILLE John Tim[2], STRAIT Edward[2], TURNBULL Alan[2], WALKER Michael[2] and DIII-D Team[2]

Princeton Plasma Physics Laboratory, Princeton, New Jersey

[1] Columbia University, New York, New York

[2] General Atomics, P.O. Box 85608, San Diego, California 92186-5608

[3] Oak Ridge National Laboratory, Oak Ridge, Tennessee

(Received: 11 December 2001 / Accepted: 24 May 2002)

Abstract

High beta plasmas with twice of the no-wall ideal kink limit have been achieved in DIII-D device by sustaining the plasma rotation. The most important element is the control of the resonant phenomena of residual error field which excites the stable resistive wall mode near the marginally stable condition (Resonant Field Amplification).

Keywords:

external kink, resistive wall mode, ideal MHD, error field

1. Introduction

The external kink mode has been considered as one of most dangerous obstacles which may hinder us from achieving commercially-attractive fusion reactors. The efficacy of the conducting shell has been demonstrated in early tokamaks, and RFPs. The presence of a conducting shell reduces the growth rate and the shell-stabilized plasmas transiently have achieved higher beta [1-3]. Since the wall with finite resistivity loses the flux-conserving stabilizing force in time, the external kink instability is branched into the resistive wall mode (RWM) [4]. Since the RWM mode exhibits a sufficiently slow growth rate, various approaches are possible to suppress or control the mode amplitude. Over the last decades, the magnetic feedback stabilization has been considered as a possible cure even in reactor oriented devices [5]. Recently a scheme with the plasma rotation through kinetic dissipation has been proposed as an alternative [6,7]. These approaches are shown schematically in Fig. 1. Recent experiments in DIII-D have shown the feasibility of both feedback stabilization [8] and rotational stabilization [9].

On the DIII-D device, it has been discovered that both magnetic feedback and rotation stabilization successfully function in a synergetic manner to reduce the RWM amplitude, maintain the plasma rotation, and establish a high $\beta_N = \beta/(B_T/aI_P)$ configuration (where the β is the ratio of plasma pressure to the toroidal magnetic pressure). A key factor is the discovery of excitation of stable RWMs by a residual error field [9,10] (Resonant Field Amplification), predicted by Boozer [11]. Near the marginal condition, the residual error field excites the stable RWM in a helically-resonant manner, causing the growth of the RWM resulting in a strong drag on the plasma rotation due to electro-magnetic torque [12,13]. Feedback which senses the mode is found not only to reduce the mode amplitude, but also compensate the resonant component of the error field. When the plasma rotation is maintained above a critical value with

Corresponding author's e-mail: mokabaya@pobox.pppl.gov

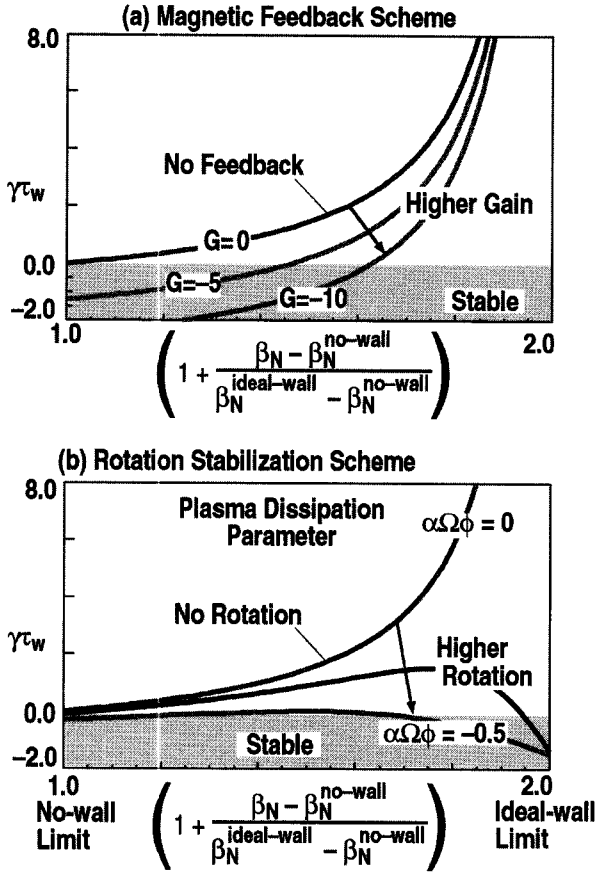

Fig. 1 Schematic diagrams of RWM stabilization. (a) Rotational stabilization without magnetic feedback. (b) Magnetic feedback stabilization with a control logic "smart shell". $\beta_N/\beta_N^{no\,wall}$ = 1.0 corresponds to the no-wall limit and $\beta_N/\beta_N^{no\,wall}$ = 2.0 corresponds to the ideal-wall limit.

sufficient angular momentum input sustained, the RWM is stabilized, which is consistent with a mechanism as discussed by Bondeson and Ward [6,7].

The improvement via maintaining the plasma rotation is obtainable in wide rage of plasma parameters such as quasi-steady state high β_N discharges [14]. The study with the MARS simulation code by [15,16] supports the observed feedback sensor preference.

In this paper, we have summarized the recent progress of RWM control on the DIII-D device.

2. Resistive Wall Mode and Error Field Amplification

2.1 Mode characteristics of RWM

The RWM is assumed to have a global helical displacement extending from the core plasma to beyond the vacuum vessel. The existence of ideal kink nature over so long a time scale (≫ Alfvénic time) seems like an over simplified hypothesis. This seemingly puzzling character based on conventional ideal MHD predictions has necessitated series of experimental, theoretical, and numerical studies.

To address the issue of the mode structure under the influence of finite resistivity, theoretical and experimental efforts have been made during last a few years. A numerical study has been carried out with the GATO and DCON plasma stability code combined with the VACUUM code [17,18]. In these analyses, the resistive flux loss on the wall and its impact back to the plasma surface is treated in a self-consistent manner. The results indicate that the mode structure inside the plasma remains largely intact and that the eddy current pattern on the wall is not significantly modified [8,12,17,18]. On the DIII-D device, the mode structure has been studied with both a high resolution ECE spectrometer and two toroidally-separated soft x-ray arrays. The results indicate that the RWM evolves in time without creating any noticeable magnetic islands even when the mode amplitude observed outside the vessel reaches to the order of 5–10 gauss [8,10,13]. The slow time evolution of the observed mode inside the plasma coincides well with the flux time history observed outside the vacuum vessel. In addition, the radial flux measured at above/below mid-plane compared with the flux evolution at the mid-plane indicates that the mode behaves as one large rigid displacement with a helicity conserved.

Bondeson and Ward [6,7] proposed that the RWM can be stabilized by the dissipation due to plasma rotation if the plasma rotation is above a critical value, typically, a few percent of Alfvénic velocity. DIII-D experiments have revealed that rapid RWM growth is coincided with sharp decrease of plasma rotation [12,19,20]. With higher angular momentum injection [8-10], the plasma rotation was increased while holding the total stored energy constant at a plasma pressure just above the no-wall beta limit. When the plasma rotation was increased by 20%, the RWM onset was delayed by 100–200ms. However, the RWM eventually grew and led to the beta collapse, indicating that the higher rotation alone was not sufficient for complete stabilization. Nonetheless, this experimental result suggests that plasma rotation is a major factor in achieving RWM control.

2.2 Resonant Field Amplification (RFA)

Boozer [11] proposed that when a plasma

approaches the marginal stability condition, namely, the no-wall beta limit against the external kink, the amplitude of the plasma distortion to a resonant component of residual external perturbation (such as error field) increases inversely proportional to a torque parameter, plasma toroidal rotation. This effect has been termed resonant field amplification (RFA).

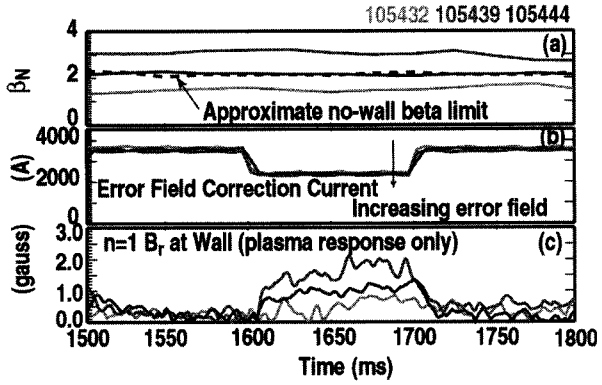

Fig. 2 Stable resistive wall mode excited with pulse field. The larger amplitude of RFA is induced with $\beta_N/\beta_N^{no\ wall} \geq 1.0$. Decay of the mode after the pulse field indicates that the plasma condition belongs to the stable regime. (a) β_N vs. time; (b) Non-axisymmetric field correction current vs. time. (c) The plasma response observed on the external δB_r saddle loop.

Experimentally it was demonstrated [9] that when β_N approaches the marginal condition, the applied pulsed error field can induce the n=1 helical response (Fig. 2). With β_N above the no-wall beta limit, $\beta_N^{no\ wall}$, the distortion is larger compared with the response at $\beta_N \approx \beta_N^{no\ wall}$. After the pulsed field was turned off, the mode decayed at the rate of $1/\tau_w$, indicating that the mode excited did belong to marginally stable regime. Figure 3(a,b) shows the RFA amplitude and phase for various β_N summarized from the pulsed field operation. Here, the RFA amplitude is defined as the helical n=1 flux due to the plasma perturbation, namely the total observed flux subtracted by the applied external field. The most important result is that there is a finite phase shift between the applied field and the excited mode. The phase shift is 20 degrees at $\beta_N \approx \beta_N^{no\ wall}$ and increases to 90–120 degrees at higher β_N. This toroidal phase shift of the plasma response should be taken into account for feedback operation. When a larger extra n=1 field is applied, the plasma rotation gradually decreases and once the velocity is below a critical value, the RFA becomes too strong, leading to rotational collapse. This indicates that the rotational stabilization requires a critical rotational velocity, which corresponds to ≈6 kHz for the present experimental condition. This value is not far from a critical velocity estimate given by [6,7] as shown later.

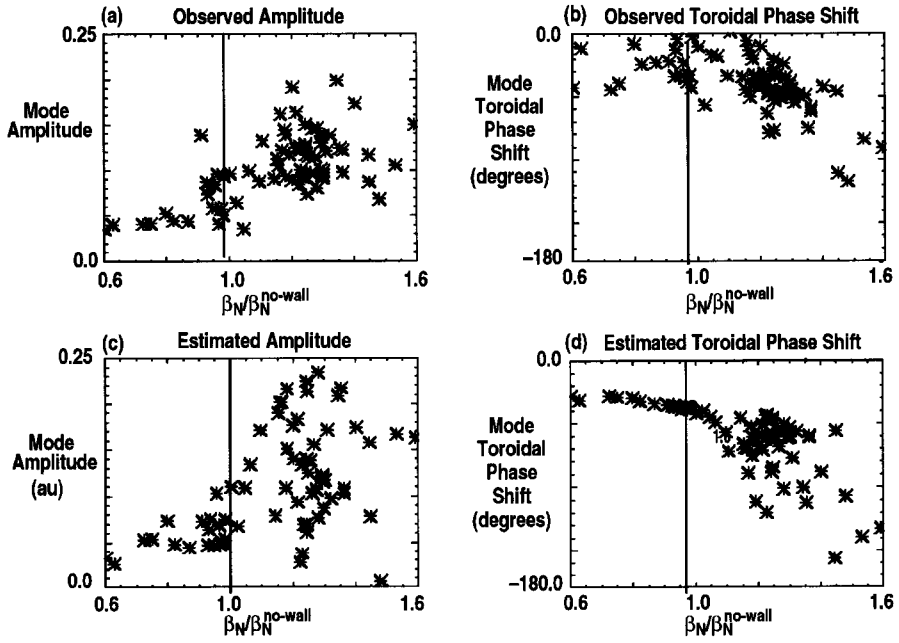

Fig. 3 RFA amplitude and toroidal phase (a) and (b): Experimental results. (c) and (d): Estimated values by eq. (4) using the observed rotation velocity. The amplitude scale is in arbitrary unit.

3. Hardware for RWM Control on DIII-D Device

The power supply required for magnetic feedback is rather modest, since the RWM growth time is of the order of the resistive wall skin time τ_w, which is far slower than the Alfvénic time. The sensor geometry depends on the choice of control logic. The smart shell scheme is to control the total flux (including the flux supplied from the coil) by compensating the helical flux leakage of the wall and to build the virtual ideal shell on the wall [5]. The smart shell approach works best with δB_r saddle loop, which detects the flux decay over the shell surface. Another scheme is the mode control logic using the signal originating only from the plasma surface displacement and without coupling to the active coil current. The mode control logic works best with poloidal field sensors inside the vacuum vessel.

On DIII-D, various sensors have been installed inside and outside the vessel. Figure 4 shows a schematic diagram of sensor and active coil location. Each saddle loop covers 60 toroidal degrees. The input signal to the feedback system is made by combining a pair of sensors located at toroidally opposed angles, to produce only n = odd components.

The active coils on DIII-D device have two roles: one is to compensate the error field and the other is to serve as the active feedback actuator. Present active coils are toroidally located in phase to the saddle flux loops. Coils located 180 degrees apart are also paired in anti-series so that only n=odd components are produced and are energized with current power supplies up to 5kA with DC-100Hz capability. A coil current of 1kA produces 13 gauss radial field on the vacuum vessel. As shown later, about one half of the maximum current is used for error field correction. It should be noted that the applied active field does not have any helicity preference, since only one layer of coil exists in the poloidal direction.

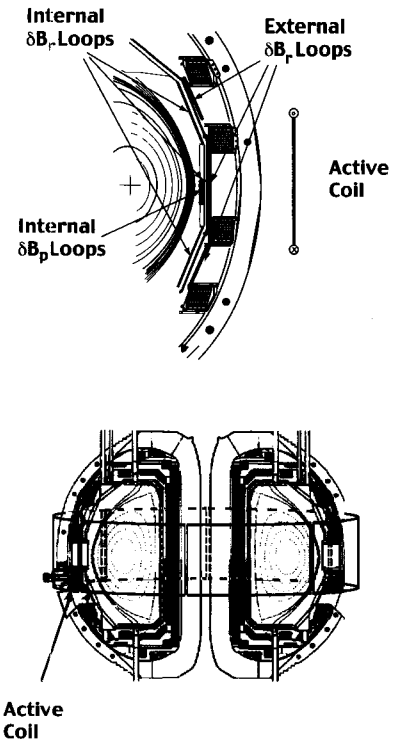

Fig. 4 Active coil geometry and sensor locations.

The possible performance of these sensors along with control logic has been analyzed with the VALEN code [21] with present coils and possible future upgrade coil locations. Best performance is obtained with the δB_p Mirnov loops located inside the vacuum vessel and the performance with δB_r saddle flux loop located outside the vacuum vessel is predicted to be less effective. The VALEN ccode also predicts that the addition of coils located above/below the midplane with δB_p sensor operation should be able to stabilize the RWM up to a value of β_N that is 90% above the $\beta_N^{\text{no wall}}$ and 10% below the $\beta_N^{\text{ideal wall}}$ limit. These results are consistent with other studies by Liu [16] and Chu [17,18].

4. Experimental Results of RWM Control

4.1 Comparison of various feedback sensors

The comparison of δB_r and δB_p located inside the vessel is shown in Fig. 5. The advantages of δB_p sensor is the rejection of δB_r component produced by either the active coil or the eddy current excited by the active coil. In this series of experiments, the discharge loses the high beta period at 1380ms. The δB_p sensor operation extended the discharge to 1580ms compared to 1440ms with the δB_r sensor. Since the q-edge was decreasing toward 3, the longer duration means that the discharge faces stronger external kink onset. The requested coil current amplitude and phase of n=1 pattern are shown in Fig. 5(c,d).

The error field correction was set 2kA to compensate approximately empirically-determined error field. For the operation of both sensors, the amplitude requested from the feedback stays at approximately 2kA level, which indicates that the initial estimated coil current was reasonable. However, δB_p sensor shifted the field direction of n=1 about 10–20 degrees immediately after the feedback was turned on. On the other hand, the δB_r sensor did not sense the need for the directional shift. The slight increase of amplitude around 1400ms

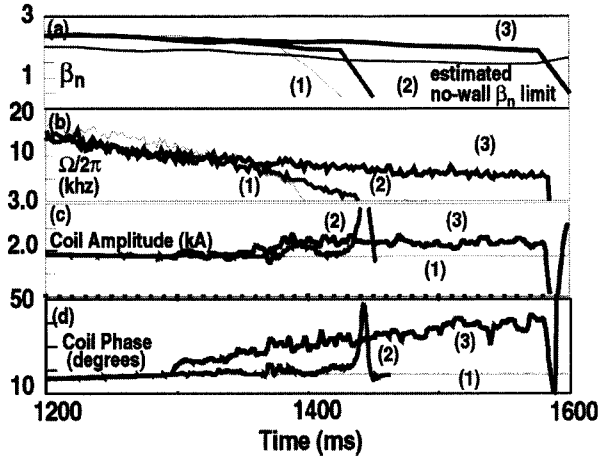

Fig. 5 Comparison of δB_r and δB_p sensors located inside the vessel. (1) Shot (106196) with no feedback, (2) Shot (106187) with the internal δB_r sensor feedback, (3) Shot (106193) with the internal δB_p sensor feedback (a) β_N and l_i (b) Rotation frequency at q = 2 surface (c) Coil current amplitude for the n=1 component (d) Coil current toroidal phase for the n=1 component.

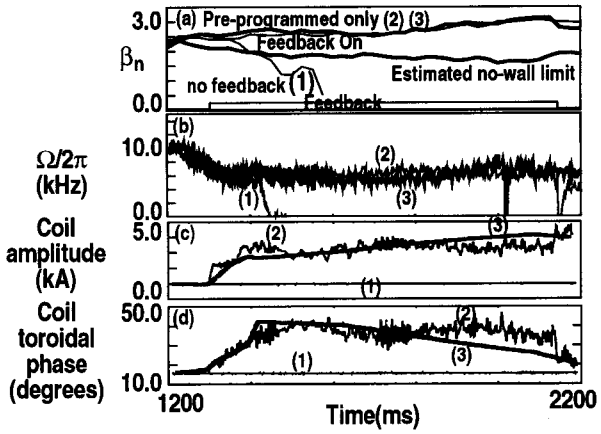

Fig. 6 Comparison with/without optimized error compensation. (1) Shot with no feedback (106530) with pre-programmed non-optimized error correction current (with amplitude of 1kA and ϕ_c = 7 degrees). (2) Shot with feedback (106532) with pre-programmed non-optimized error correction current (amplitude of 1kA and ϕ_c = 7 degrees). (3) Shot with feedback shot (106534) with pre-programmed error correction current adapted from the feedback shot (106532) (a) β_N and estimated limit, (b) Plasma rotation frequency at q = 3 surface, (c) coil current amplitude for the n=1 component, (d) Coil current toroidal phase for the n=1 component.

could not stabilize the mode, leading to the final collapse. The fine detection of field direction and its adjustment seem to have been the crucial element for stabilizing the RWM.

4.2 High β_N achievement via error field correction by feedback

Once it was determined that the δB_p sensor is superior to other sensors, the long-duration, high β_N, discharge was explored using the internal δB_p sensor. The target discharge was with a modest I_p ramp of 0.6MA/s. Without feedback the preprogrammed current for error field correction was set to 1kA with ϕ_c = 7 degrees (Fig. 6). The rotation velocity started to decrease rapidly, similar to the case in Fig. 6, due to the increase of the RWM and the β_N decreased gradually from 1300ms (case 1). When the feedback was applied with the same pre-programmed current, the feedback increased immediately the coil current to 2kA and gradually up to 3–4kA level and the field direction was shifted to ϕ_c = 40 degrees. The high beta duration was increased to 2000ms together with β_N increase to 3.0, which is about twice of $\beta_N^{\text{no wall}}$ and close to according to $\beta_N^{\text{ideal wall}}$ GATO calculation (case 2). When the pre-programmed current was modified to match the coil current obtained by feedback operation (case 2), the time evolution of β_N is identical to the feedback (case 2), and the plasma rotation velocity is also very similar to the results obtained with feedback (case 3).

The comparison of these three types of operations indicates that (1) the feedback process can track the error field with good accuracy, and as a consequence, the n=1 component of error field was determined with the feedback process and (2) the use of the obtained current as error field correction without feedback can produce the high plasma rotation velocity and high b^N configuration. This observation along with discussion in Sec. 2 on high β_N achievement with higher angular momentum indicates that the higher rotation velocity with better error field correction is the essence of this success.

5. Advancing the RWM Control Concept

These experimental results indicate that magnetic feedback stabilization and stabilization by plasma rotation are not two distinct processes, but that both of them work together in a tightly coupled manner as shown in Fig. 7.

Recently, theoretical studies have been carried out on the RWM process including plasma rotation by several groups [22-25]. The overall feedback process can be described qualitatively with a cylindrical lumped

model as was discussed in [26]. The main parameter is, L_{eff}, which can represent the pressure balance and the normal magnetic field continuity at the plasma surface.

$$L_{eff}\delta I_p + C_{wp}\delta I_w + C_{cp}\delta I_c = 0 \qquad (1)$$

where, suffixes p, w, c, and o correspond to plasma, passive wall, external (active or error field) coil, and observation sensor respectively. The C_{ij} are mutual inductances between these elements. δI_p, δI_w, and δI_c correspond to the plasma skin current, the passive wall eddy current, and the external coil current respectively. The value, L_{eff}, includes the MHD mode displacement gradient, β_o, defined just inside the plasma surface, and the safety factor through $f = m - nq$. The formulation can be expanded in order to include the dissipation of the mode due to the plasma rotation and kinetic term for low frequency limit ($\gamma\tau_A < 1$),

$$L_{eff} = (\beta_o - 2/f + 1 + \kappa\Omega_\phi^2 + i\,\alpha\Omega_\phi)/$$
$$(\beta_o - 2/f - 1 + \kappa\Omega_\phi^2 + i\,\alpha\Omega_\phi) \qquad (2).$$

where, the value, Ω_ϕ, is the angular rotational frequency and κ, and α represents the strength of kinetic, and dissipation term relative to the plasma potential energy

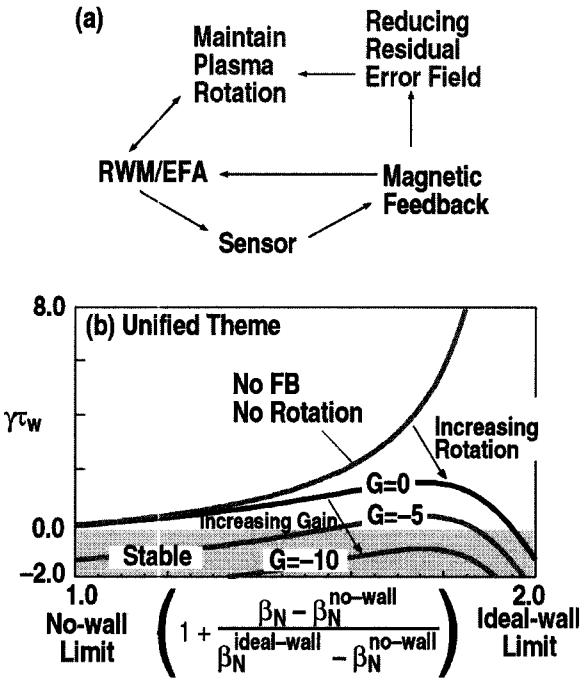

Fig. 7 Schematic of unified theme for RWM control both with feedback and plasma rotation. (a) The performance with the unified theme and (b) Schematic diagram.

respectively. This formulation is equivalent to the treatment of the kinetic energy and dissipation term with δw approach in the [24]

$$(\gamma\tau_w + i\Omega_\phi\tau_w)^2(\kappa/\tau_w^2) + (\gamma\tau_w + i\Omega_\phi\tau_w)(\alpha/\tau_w)$$
$$+ \delta W_p + (\delta W_v^b\gamma\tau_w + \delta W_v^\infty)/(\gamma\tau_w + 1) = 0 \qquad (3)$$

where, the first and second terms represent the impact of plasma rotation and dissipation, and the third term the ideal MHD potential energy. The fourth term is for the effect of finite wall resistivity.

When an external field such as error field exists, the plasma mode response in the quasi steady state is given by

$$\delta I_p = (-C_{cp}/L_{eff})\,\delta I_c\,. \qquad (4)$$

This simple cylindrical formulation is obtained for a current kink driven RWM with $f_{min} < f \le 1$ where f=1 and f=f_{min} correspond to current driven kink onset with no-wall and with ideal wall respectively. The model does not include the value β_N. However, we still can discuss the qualitative behavior by relating β_N to f with $\beta_N = 2/f - 1$, when the plasma condition approaches the ideal MHD limit. With this definition, we preserve the fundamental criterion: f=1 as the marginal stability condition for ideal kinks at $\beta_N = \beta_N^{no\ wall}$ and the usual wall-plasma separation determines f_{min} (<1) at $\beta_N = \beta_N^{ideal\ wall}$. A similar relation is also used in [21,27].

Figures 3(c) and (d) show the estimated values for the observed RFA using β_o = 1.3, α = 0.002, κ = 0, and experimentally observed plasma rotation. The absolute value of the mode amplitude can not be estimated from the cylindrical mode, mainly due to the limitations imposed by the single pattern assumption in this simple cylindrical model, causing a mismatch of field patterns between the externally-applied and mode fields. The estimated dependence of the toroidal phase shift versus, $\beta_N/\beta_N^{no\ wall}$ seems to be qualitatively consistent with the observations. The large scattering on the estimated values of amplitude and phase can be attributed to too-high of a sensitivity due to the resonant condition and to the uncertainty of the rotational frequency. However, this scattering itself may reflect the hidden parameters of the actual dissipation mechanism, of which details are not included in this simple model.

For completeness in modeling the feedback scheme shown in Fig. 8(a), the time behavior of the plasma rotation must be included. Here, we will use the angular momentum dissipation equation with the electromagnetic torque applied by the external field to the

mode on the plasma surface [22,23,25,28] expressed using the lumped parameter approach [26] instead of the commonly used flux discontinuity on the plasma surface.

$$\tau_w^2 \partial/\partial t(\Omega_\phi) = C_N^{rot}\, \delta I_p\, (C_{pw}\, \delta I_w + C_{pc}\, \delta I_c)$$
$$[\delta I_p(0)\, \delta I_c(0)]^{-1}\, (C_{pw} C_{pc})^{-1/2} \qquad (5)$$

where, $C_N^{rot} = 2\pi\, (a/R)[\tau_w^2 \partial(\tau_A^{\delta B-p}\, \tau_A^{\delta B-ext})$, and time is normalized to τ_w.

Here, $\tau_A^{\delta B-p}$ and $\tau_A^{\delta B-ext}$ are Alfvén times for magnetic field on the plasma surface produced by $\delta I_p(t=0)$ and $\delta I_c(t=0)$ respectively.

The shell boundary condition provides

$$C_{pw} \partial/\partial t(\delta I_p) + L_w \partial/\partial t(\delta I_w) + C_{wc} \partial/\partial t(\delta I_c) + R_c \delta I_w = 0. \qquad (6)$$

The active coil current, δI_c, with a current power supply provides

$$\delta I_c = G\, \delta \Psi_0,\ \delta \Psi_0 = C_{op}(\delta I_p) + C_{ow}\, (\delta I_w) + C_{wc}\, (\delta I_c). \qquad (7)$$

Equations (2), (5), and (6) correspond to the MHD equations formulated in [23] in the limit of slow time evolution.

The model with eqs. (2), (6) and (7) was used to calculate the stabilizing effects of rotation and feedback, as shown earlier in Fig. 1. It is important to note that each method has its limitations. Feedback alone [Fig. 1(b)] leads to a stability limit below the ideal-wall limit. Plasmas stabilized by rotation alone may be only weakly stable over a large range of beta values [Fig. 1(a)] and are vulnerable to error fields. However, the model also shows that the combination of rotation and feedback can yield robust stabilization up to the ideal-wall limit.

6. Summary

We have made substantial progress in the control of one of most dangerous MHD modes for practical rectors, the resistive wall mode. Open loop operation discovered that at $\beta_N \approx \beta_N^{no\ wall}$, the marginally stable RWM responds in a resonant manner to the applied field with the toroidal phase shift relative to the applied field as predicted by Boozer. The accurate tracking of the residual error field took place through the feedback process. When sufficient angular momentum injection is available, $\beta_N \approx \beta_N^{ideal\ wall}$, can be achieved by sustaining the plasma rotation.

A simple simulation can provide qualitative behavior of RFA and the feedback operation. This indicates that, although the RWM feedback process is complex, a few fundamental parameters may play significant roles on the process.

7. Acknowledgments

This work is supported by U.S. Department of Energy Grant DE-FG02-89ER53297 and Contracts DE-AC03-99ER54463, DE-AC05-00OR22725, and DE-AC02-76H03073. We are greatly thankful to physicists, engineering staffs, technical staffs involved in this project. In particular, we would like to express our appreciation to DIII-D operation group.

References

[1] T.S. Taylor, *et al.*, Phys. Plasmas **2**, 2390 (1995).
[2] M. Okabayashi, *et al.*, Nucl. Fusion **36**, 1167 (1996).
[3] T. Ivers, *et al.*, Phys. Plasmas **3**, 1926 (1996).
[4] J. Freidberg, *Ideal Magneto-Hydro-dymanics* (Plenum, New York, 1987), Chapter 9.
[5.] R. Fitzpatrick and T. Jensen, Phys. Plasmas **2**, 2641 (1996).
[6] A. Bondeson and D. Ward, Phys. Rev. Lett. **72**, (1994) 2709.
[7] D.J. Ward and A. Bondeson, Phys. Plasmas **2**, 1570(1995)
[8] M. Okabayashi *et al.*, Phys. Plasmas **8**, 2071 (2001).
[9] A.M. Garofalo *et al.*, Phy. Plasmas (APS invited paper, accepted); A.M. Garofalo, R.J. La Haye, and J.T. Scoville, "I need a title here," to be submitted to Nucl. Fusion.
[10] A.M. Garofalo *et al.*, Nucl. Fusion **41**, 1171 (2001).
[11] A. Boozer, Phy. Rev. Lett. **86**, 1176 (2001).
[12] A.M. Garofalo *et al.*, Phys. Rev. Lett. **82**, 3811 (1999).
[13] L. Johnson *et al.*, in "Structure and Feedback Stabilization of Resistive Wall Modes in DIII-D," in Proc. of the 28th EPS Conf. on Controlled Fusion and Plasma Physics, Madeira, 2001 (European Physical Society, Petit-Lancy, 2001) to be published.
[14] M.R. Wade "Physics of High Bootstrap Fraction, High Performance Plasmas on the DIII-D Tokamak," in Proc. of the 28th EPS Conf. on Controlled Fusion and Plasma Physics, Madeira, 2001 (European Physical Society, Petit-Lancy, 2001) to be published.
[15] Y.O. Liu and A. Bondeson, Phys. Rev. Lett. **84**, 907 (2000).

[16] Y.Q. Liu, *et al.*, Phys. Plasmas **7**, 3681 (2000).
[17] M.S. Chu *et al.*, "Modeling of Feedback Stabilization of the Resistive Wall Mode in General Geometry," in Proc. of the 28th EPS Conf. on Controlled Fusion and Plasma Physics, Madeira, 2001 (European Physical Society, Petit-Lancy, 2001) to be published.
[18] M.S. Chance *et al.*, "Theoretical Modeling of the Feedback Stabilization of External MHD Modes in Toroidal Geometry," Nucl. Fusion (accepted).
[19] E.J. Strait *et al.*, Phys. Rev. Lett. **74**, 2483 (1994).
[20] A.M. Garofalo, *et al.*, Nucl. Fusion **40**, 1491 (2000).
[21] J. Bialek *et al.*, Phys. Plasmas **8**, 2170 (2001).
[22] R. Fitzpatrick and A. Aydmir, Nucl. Fusion **36**, 11 (1996).
[23] R. Fizpatrick, "A Simple Model of the Resistive Wall Mode in Tokamaks," (private communication).
[24] M.S. Chu *et al.*, Phys. Plasmas **2**, 2236 (1995).
[25] A. Boozer, Phys. Plasmas **6**, 3180 (1999).
[26] M. Okabayashi, N. Pomphrey and R. Hatcher, Nucl. Fusion **38**, 1607 (1998).
[27] A. Boozer, Phys. Plasmas **9**, 3350 (1998).
[28] S.C. Guo and M.S. Chu, Phys. Plasmas **8**, 3342 (2001).